SCIENTIFIC PAPERS
OF THE UNIVERSITY OF PARDUBICE
Series A
Faculty of Chemical Technology
11 (2005)

EFFECT OF LIQUID RHEOLOGICAL BEHAVIOUR ON BATCH SEDIMENTATION OF COARSE SPHERICAL PARTICLES

Bedřich ŠIŠKA[a], Ludmila MACHAČOVÁ[b] and Ivan MACHAČ[a1]
[a]Department of Chemical Engineering, [b]Department of Mathematics,
The University of Pardubice, CZ–532 10 Pardubice

Received September 30, 2005

An experimental study of influence of liquid rheological behaviour on batch sedimentation of coarse spherical particle suspensions is presented. In the experiments, the sedimentation course of assembles of spherical particles settling in a Plexiglas column of rectangular cross-section ("two dimensional" column) in creeping flow region was video recorded and the video sequences were evaluated visually and using an image analysis. The particles used were closely monodispersed glass spheres of diameter 1.92 and 4.12 mm. The range of initial mean volume fraction of solid in suspensions tested was from 0.05 to 0.40. Dispersing liquids tested were aqueous solutions of glycerol (Newtonian fluid) and solutions of methylcellulose Tylose MH 4000, hydroxyethylcellulose Natrosol 250 MR, and polyethylene oxide Polyox WSR 301. The basic tool used for image processing and analysis was commercially available software Screen Measurement M. The creation of different zones of particles was detected during

[1] To whom correspondence should be addressed.

sedimentation. The form and time development of these zones depend on the rheological behaviour of the fluid, particle diameter, and initial concentration of suspension.

Introduction

Batch sedimentation of assembles of solid particles is an industrially important process encountered in many technological applications such as, for example, clarification, thickening, and classification. Hindered sedimentation of non-flocculated homogeneous suspensions of uniform size spherical particles represents an idealisation of such a process, which is often exploited for experimental and theoretical investigation of sedimentation principles.

Great effort has been put into the investigation of sedimentation in Newtonian fluids and the fundamentals of this operation are described in numerous monographs and textbooks (e.g. [1]). As a basis of description of batch sedimentation of solid particles in Newtonian liquids, Kynch's analysis [2] is usually recognised. The Kynch sedimentation theory, as well as its revised versions [3,4], is based on the assumption that the particle distribution is uniform in a horizontal layer of the settling suspension.

At the same time, the settling behaviour of assembles of solid particles in non-Newtonian fluids has been subject of only a few experimental studies and remains poorly known. Existing studies in shear thinning and elastic fluids show the development of inhomogeneous structures during sedimentation that are induced by particle aggregation [5–9]. It results in a different sedimentation course as compared with that in Newtonian fluids.

In this work, the results are presented of the investigation of the batch sedimentation of the solid spherical particles settling in non-Newtonian liquids having different values of shear thinning and elasticity. In the experiments, the sedimentation course of assembles of spherical particles settling in a Plexiglas column of rectangular cross-section ("two dimensional" column) was video recorded and the video sequences were evaluated using an image analysis.

Experimental

In our experiments, the sedimentation tests of spherical particle suspensions in liquids of different rheological behaviour were performed. The experimental equipment consisted of a Plexiglas settling column of rectangular cross-section, video camera Panasonic NVS-4E, a personal computer, and lighting.

The particles used were closely monodispersed glass spheres of diameters 1.92 and 4.12 mm. Their density was 2524 and 2596 kg m^{-3}. The range of initial

mean volume fraction of suspension tested ranged from 0.05 to 0.40.

The test liquids were aqueous solutions of glycerol (Newtonian fluid) and solutions of methylcellulose Tylose MH 4000, hydroxyethylcellulose Natrosol 250 MR, and polyethylene oxide Polyox WSR 301. The shear stress – shear rate data of liquids were measured (at 20 °C) on the cylindrical rheometer Rheotest II ($1.5 \leq \dot{\gamma} \leq 1200\ s^{-1}$). The material functions of the unsteady shear flows of the polymeric liquids were measured additionally on the dynamical rheometer RheoStress RS 150 [10].

Terminal falling velocities of test particles were measured in three Plexiglas cylindrical columns of 20, 40, and 80 mm in diameter and 1 m length (to evaluate the effect of the container walls). The reached Reynolds numbers $Re_{tn} \approx Re_{tC}$ ranged from 0.0036 to 0.1 (creeping flow regime).

The dimensions of the settling column were 530 mm in height, 80 mm in width, and 12 mm in depth. Two fluorescent tubes were used for side lighting of working area.

The sedimentation tests were performed at room temperature (20 ± 0.5 °C). At first, the settling column was filled with investigated liquid having the desired temperature. After disengaging of incidentally trapped air bubbles, the corresponding amount of glass spheres, wetted beforehand in the test fluid, was inserted into the settling column. Next, the column was mounted into a vertical frame rotated about the horizontal axis to disperse solids and to achieve nearly homogeneous suspension. After achieving the particle dispersion, the column rotation was stopped at a vertical position and the course of particle sedimentation was observed and recorded by the video camera. Each test with the same initial suspension concentration was repeated three times.

The basic tool used for image processing and analysis was commercially available software Screen Measurement M, supplied by Laboratory Imaging Ltd. The software allowed the recording, threshold setting, intensity measurements, filtering, identification, counting, and measurement of objects in a digitised image. The procedures used for image analysis are described in detail in Ref. [7].

Results and Discussion

Rheological Characteristic of Test Fluids

From the shear stress – shear rate data, parameters K and n of the power law

$$\eta(\dot{\gamma}) = K\dot{\gamma}^{n-1} \tag{1}$$

and parameters η_0, λ and m of the Carreau viscosity model

$$\eta(\dot{\gamma}) = \frac{\eta_0}{[1 + (\lambda\dot{\gamma})^2]^{(1-m)/2}} \quad (2)$$

were determined. The characteristics of test liquids are summarized in Table I. The solution of glycerol is a Newtonian fluid, polymer solutions exhibit different degree of shear thinning and elasticity. The measure of shear thinning increases with the decreasing values of parameters n or m. Making use of tests of linear elasticity [10], it was verified that the relative measure of polymer solution elasticity can be roughly estimated according to the value of the time parameter λ of the Carreau model. In accordance with that, the solution of Tylose is nearly inelastic, the solution of Natrosol is mildly elastic, and the solution of Polyox is highly elastic.

Table I Characteristics of the test liquids, 20 °C

Liquid	ρ kg m^{-3}	n	K Pa s^n	$\dot{\gamma}$ s^{-1}	η_0 Pa s	λ s	m
Glycerol 99 %	1260	1	1.323	-	1.323	0	1
Tylose 1.4 %	1003	0.825	0.672	1.5 – 8.1	0.483	0.057	0.695
Natrosol 1.6 %	1004	0.717	2.22	1.5 – 16	1.769	0.180	0.509
Polyox 0.8 %	999	0.446	1.499	1.5 – 16	4.446	4.47	0.467

Sedimentation Experiments

Quality of Sedimentation

From the video records of individual sedimentation tests, the development of the structure of settling beds has been compared. The examples of video sequences of sedimentation tests in different fluids are shown for sedimentation of particles of diameter 1.92 mm for mean volume fractions of solids 0.10 – 0.20 in Figs 1 – 3.

It was verified that the sedimentation in the Newtonian fluid (glycerol) is nearly homogeneous. The creation of four zones can be observed during sedimentation: the zone of clear fluid, the zone containing relatively isolated particles, the zone with nearly constant particle concentration approximately equal

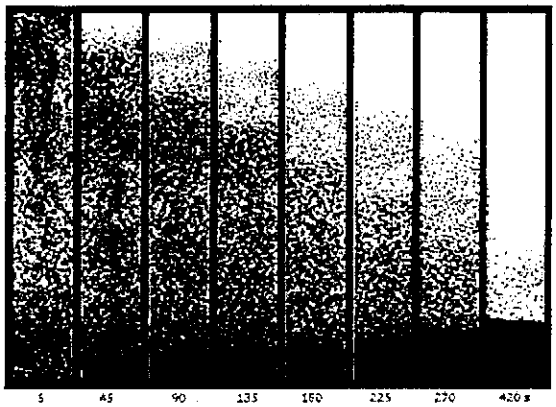

Fig. 1 Time behaviour of sedimentation of spheres of 1.92 mm in glycerol at initial volume fraction 0.10

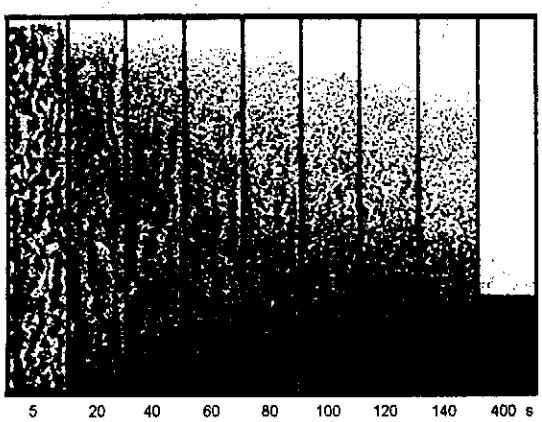

Fig. 2 Time behaviour of sedimentation of spheres of 1.92 mm in Natrosol at initial volume fraction 0.15

to the initial one, and the zone of sediment (Fig. 1). At the same time, the way of creation of zones depends on the initial concentration of suspension. The sharp interface between second and third zones has been visually detected only during sedimentation of more concentrated suspensions ($c_{v0} \geq 0.15$).

The sedimentation course of suspensions of particles in solution of Tylose was analogous to that in solution of glycerol. In this case, the weak shear thinning and very weak elastic behaviour of the fluid evidently does not affect the sedimentation course.

In contrast to the foregoing cases, the sedimentation in moderately shear thinning and elastic solution of Natrosol is already markedly aggregative. At the beginning of the sedimentation, the clusters of particles are created along with

liquid channels and cavities. The cluster size and form depend on suspension concentration and dimension of particles. In sedimentation of more concentrated suspensions of smaller particles, the clusters are longitudinal, relatively quickly settle and above them a zone of more slowly settling particles is formed (Fig. 2). At the top of this zone, a cloud of individual particles is developing.

The sedimentation in highly elastic solution of Polyox is intensively aggregative (Fig. 3). Analogous to the sedimentation in solution of Natrosol, the size and form of created clusters depend on suspension concentration and dimension of particles. At the beginning of the sedimentation, the particles swiftly organize into quickly settling vertical ligaments which are gradually turning into individual particle chains. The vertical structures fade away and the remaining particles slowly settle down in a dilute zone.

Fig. 3 Time behaviour of sedimentation of spheres of 1.92 mm in Polyox at initial volume fraction 0.20

Concentration Profiles

Making use of the function Mean grey of the software Screen Measurement [7], the dependences of the mean suspension concentration c_v on the distance h from the bottom of the column and on the sedimentation time t were evaluated. The results obtained confirm that during sedimentation in Newtonian solution of glycerol the concentration c_v of particles in the main settling zone does not essentially depend on the distance h and is approximately equal to c_{v0} (see Fig. 4).

Along with the increasing shear thinning and elasticity of the liquid, the concentration c_v in the main settling zone decreases with increasing value of h and $c_v > c_{v0}$ (see Figs 5 and 6).

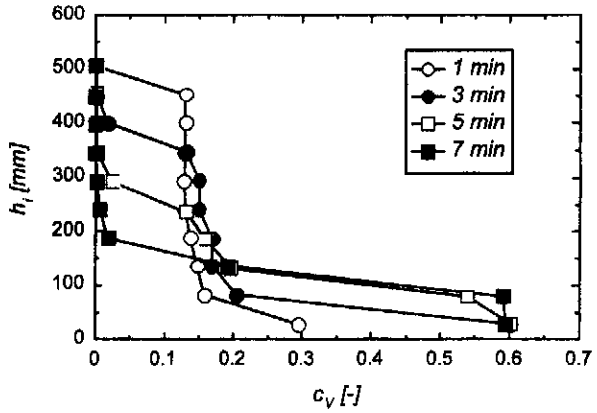

Fig. 4 Concentration profiles for batch sedimentation of spheres of 1.92 mm in glycerol at initial volume fraction 0.15

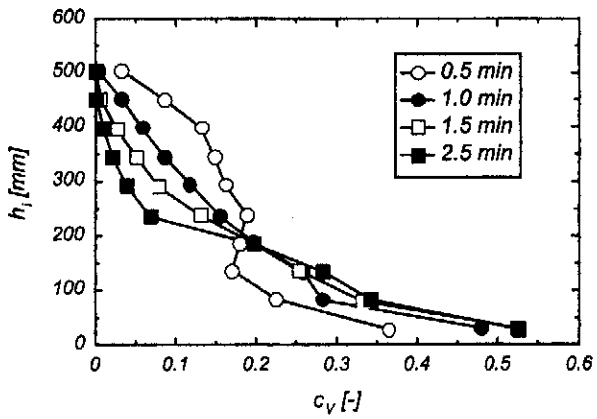

Fig. 5 Concentration profiles for batch sedimentation of spheres of 1.92 mm in Natrosol at initial volume fraction 0.15

Sedimentation Velocity

From the course of sedimentation curves (dependences of the height h_l of the interface of the clear liquid and suspension on the time t), the dependences of non-dimensional sedimentation velocity $u_B = u_s/u_t$ on the concentration c_v of suspension were determined using the Kynch procedure [1,7].

The sedimentation curves were evaluated from video sequences of individual sedimentation tests visually or by the image analysis. Their examples are given for sedimentation of spheres of diameter 1.92 mm in solutions of glycerol, Natrosol, and Polyox in Figs 7 – 9. The corresponding dependences of u_B upon c_v are shown for sedimentation in solutions of glycerol, Natrosol, and

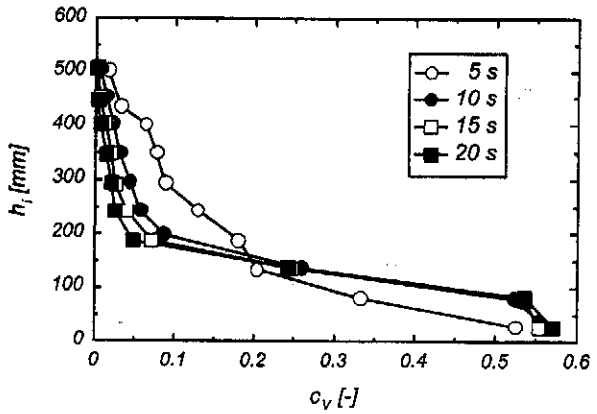

Fig. 6 Concentration profiles for batch sedimentation of spheres of 1.92 mm in Polyox at initial volume fraction 0.15.

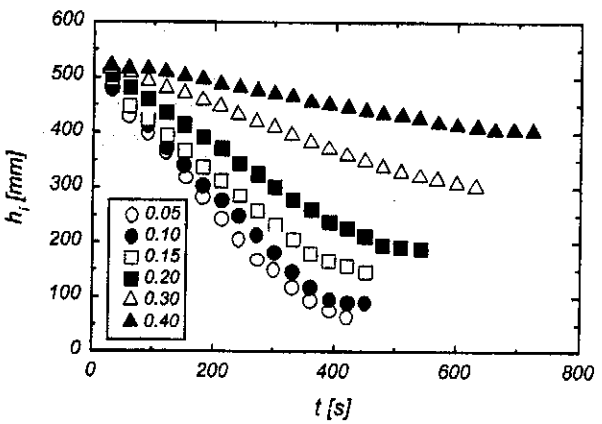

Fig. 7 Sedimentation curves for batch sedimentation of spheres of 1.92 mm in glycerol

Polyox in Figs 10 – 12. We note that the dependences obtained for sedimentation of greater particles of diameter 4.17 mm displayed a similar course.

The experimental dependences u_B upon c_v were compared with the theoretical ones, predicted making use of relationship

$$u_s = u_t \Phi(\varepsilon) \tag{3}$$

which is expected to be valid for hindered sedimentation (e.g. [1]). Here, $\varepsilon = 1 - c_v$ is the mean porosity of the suspension.

If the relative motion of particles and liquid is considered, in spite of obvious differences in the detailed flow fields, a great deal of similarity exists at a macroscopic level between the settling characteristics of a suspension and the

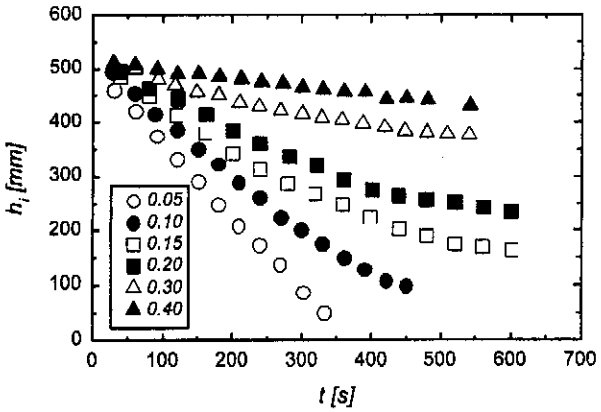

Fig. 8 Sedimentation curves for batch sedimentation of spheres of 1.92 mm in Natrosol

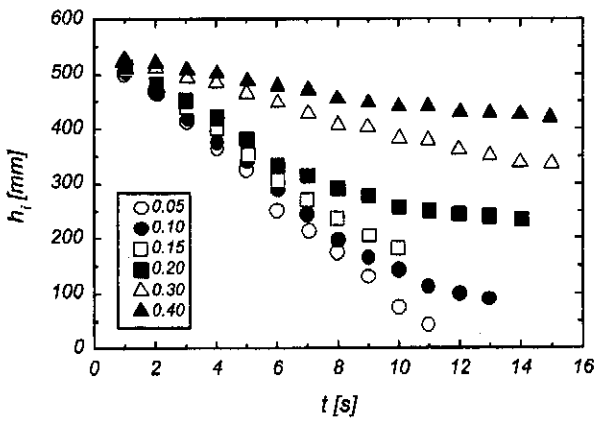

Fig. 9 Sedimentation curves for batch sedimentation of spheres of 1.92 mm in Polyox

expansion behaviour of a particularly fluidized bed of uniform size spheres. Therefore, the relationships initially developed for fluidization can also be used for the expression of the function $\Phi(\varepsilon)$ in the case of hindered sedimentation (e.g. [11]). In this work, we tested the relationship

$$\frac{u_s}{u_i} = \left(\frac{\varepsilon}{\varepsilon_i}\right)^{z_i} \tag{4}$$

suggested in Ref. [12] primarily for fluidization of spherical particle beds with polymer solutions in the creeping flow region. The form of Eq. (4) reflects the fact

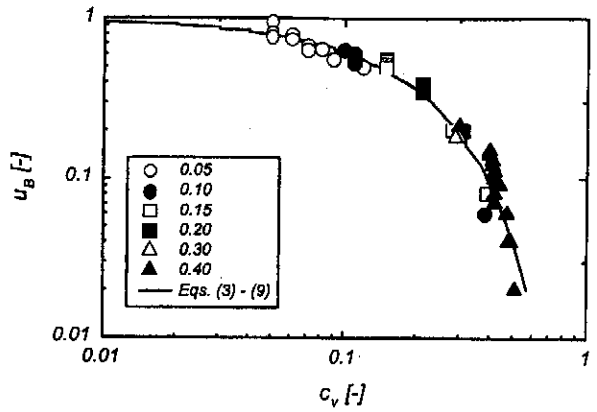

Fig. 10 Dependence of normalised sedimentation velocity u_B on solid volume fraction c_v for batch sedimentation of spheres of 1.92 mm in glycerol

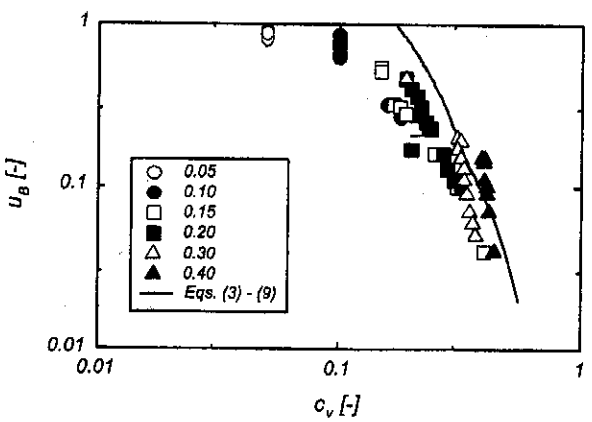

Fig. 11 Dependence of normalised sedimentation velocity u_B on solid volume fraction c_v for batch sedimentation of spheres of 1.92 mm in Natrosol

that the expansion curves displaying the dependence $\log(u/u_t) = f(\log \varepsilon)$ can be approximated by two tied straight line segments. Here (ε_i, u_i) are the coordinates of a characteristic point lying either on the bottom ($i = 1$) or on the upper segment ($i = 2$) of the expansion curve, z_i are exponents corresponding to the slopes of the bottom or of the upper straight line segment in a log-log plot. For the bottom segment [12],

$$u_1 = 0.02 u_t \tag{5}$$

and

$$\varepsilon_1 = \left(\frac{0.02}{F_W} \right)^{0.213} \tag{6}$$

where F_W is the wall effect correction factor. For the upper segment,

$$u_2 = 0.12 u_t \tag{7}$$

and the corresponding value of ε_2 can be determined from Eq. (4) for $i = 1$. For the estimation of values of the exponent z_i, the following relationships have been proposed:
for inelastic and weakly elastic fluids ($\Lambda_t < 3$, $m > 0.5$)

$$z_1 = 4.7 + 0.86(1 - m) \tag{8}$$

$$z_2 = 4.9 + 7(1 - m)\Lambda_t^{0.22} \tag{9}$$

and for more elastic fluids ($\Lambda_t > 3$, $m < 0.5$)

$$z_1 = 4.7 + 11.1(1 - m)\Lambda_t^{0.11} \tag{10}$$

$$z_2 = 8 + 34.3(1 - m)\Lambda_t^{0.16} \tag{11}$$

The calculated dependences of u_B upon $c_v = 1 - \varepsilon$ are represented by full lines in Figs 10 – 12.

Good accordance between experimental and calculated data u_B has been found for sedimentation of spherical particle suspensions in the Newtonian solution of glycerol (Fig. 10) and weakly non-Newtonian solution of Tylose. In this case the mean relative deviation δ_m of experimental and calculated data was 10 %. The values of deviations increase with the increasing liquid non-Newtonian anomaly and decreasing value of c_{v0}. For sedimentation in the moderately shear thinning and elastic solution of Natrosol, the value of δ_m was already about 30 %.

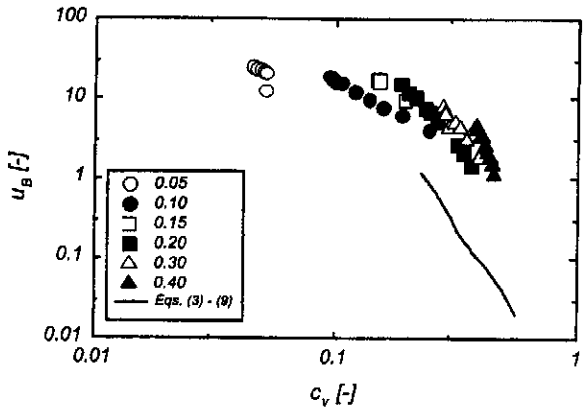

Fig. 12 Dependence of normalised sedimentation velocity u_B on solid volume fraction c_v for batch sedimentation of spheres of 1.92 mm in Polyox

The experimental values of u_B, however, do not exceed the maximum theoretical value $u_B = 1$ yet (Fig. 11). For sedimentation in the highly shear thinning and elastic solution of Polyox, we can see a dramatic disagreement between experimental and calculated data of u_B. It is evident from Fig. 12 that the experimental values of u_s exceed many times the terminal settling velocity u_t of the individual particles, which corresponds to the sedimentation of big longitudinal aggregates of particles.

The results obtained show that the function $\Phi(\varepsilon)$ proposed for fluidization can be used for correct prediction of the hindered settling velocity only for purely viscous fluids when the sedimentation is considered to be uniform. In this case, the Kynch sedimentation theory can also be applied. On the other hand, due to particle aggregation, the use of that function fails (as well as the use of the Kynch theory) in the case of sedimentation in evidently shear thinning and elastic fluids.

Conclusion

Batch sedimentation of spherical particle suspensions in Newtonian solution of glycerol and non-Newtonian polymer solutions has been investigated experimentally in a narrow column with rectangular cross-section in the creeping flow region. The time behaviour of individual sedimentation tests was video recorded and analysed both visually and using an image analysis.

The creation of different zones of particles was detected during sedimentation. The form and time development of these zones depend on the rheological behaviour of the fluid, particle diameter, and initial concentration of suspension.

In accordance with the results of previous papers dealing with the batch sedimentation in non-Newtonian fluids, the aggregation of particles was observed in the case of sedimentation in shear thinning and elastic fluids. In the strongly shear thinning and elastic fluid, particle aggregation leads to the formation of vertical particle-rich structures and of an inhomogeneous particle volume concentration along the column height. Due to these effects, the settling is more efficient within intermediate times of sedimentation. At the same time, the relationships valid for prediction of the hindered settling velocity in Newtonian suspensions fail in this case.

Symbols

c_v volume fraction of solid in the suspension
c_{v0} initial volume fraction of solid in the suspension
D column equivalent diameter, m
d sphere diameter, m
h distance from the bottom of the column, m
h_i distance of interface of clear liquid and suspension from the bottom of the column, m
K power law parameter, Pa s^n
m Carreau model parameter
n power law parameter
Re_{tC} $\left(= \frac{du_t\rho}{\eta_0}\left(1 + \Lambda_t^2\right)^{(1-m)/2} \right)$ Carreau model Reynolds number
Re_{tn} $\left(= \frac{d^n u_t^{(2-n)}\rho}{K} \right)$ power law Reynolds number
t sedimentation time, s
u_B $\left(= u_s/u_t\right)$ normalised sedimentation velocity of the suspension, m s^{-1}
u_s sedimentation velocity, m s^{-1}
u_t terminal settling velocity of particle, m s^{-1}
u_i y-coordinate of a characteristic point lying on the expansion curve, m s^{-1}
z_i exponent in Eq. (4)
$\dot{\gamma}$ shear rate, s^{-1}
δ_m mean relative deviation between experimental and calculated values of u_B
ε porosity
ε_i x-coordinate of a characteristic point lying on the expansion curve
η liquid viscosity, Pa s
η_0 Carreau viscosity model parameter (zero shear rate viscosity), Pa s
λ Carreau viscosity model time parameter, s

Λ_t ($= \lambda u_t / d$) dimensionless time parameter
ρ liquid density, kg m^{-3}

Subscripts

1 related to the bottom segment of expansion curve
2 related to the upper segment of expansion curve

References

[1] Novák V., Rieger F., Vavro K.: *Hydraulic Processes in Chemical and Food Industry* (in Czech), SNTL, Praha, 1989.
[2] Kynch G.J.: Trans. Farraday Soc. **48**, 166 (1952).
[3] Tiller F.M.: AIChE J. **27**, 823 (1981).
[4] Fitch B.: AIChE J. **29**, 940 (1983).
[5] Allen E., Uhlherr P.H.T.: J. Rheol. **33**, 627 (1989).
[6] Šiška B.: *Batch Sedimentation of Solid Particles in a non-Newtonian Liquid* (in Czech), PhD Thesis, VŠCHT Pardubice, 1994.
[7] Truhlář P.: Sedimentation of Sperical Particles in Liquids in a Column of Rectangular Cross-Section (in Czech), Diploma Work, The University of Pardubice, 1997.
[8] Bobroff S., Phillips R.J.: J. Rheol. 42, 1419 (1998).
[9] Daugan S., Talini L., Herzhaft B., Peysson Y., Allain C.: Oil Gas Sci. Technol. – Rev. IFP **59**, 71 (2004).
[10] Teichman R., Brokl P., Šiška B., Machač I.: 27th International Conference of Slovak Society of Chemical Engineering, P222, Tatranské Matliare, Slovakia, 2000.
[11] Chhabra R.P.: *Bubbles, Drops, and Particles in Non-Newtonian Fluids*. CRC Press, Boca Raton, 1993.
[12] Machač I., Bena, J., Šiška, B.: 13th International Congress of Chemical and Process Engineering CHISA '98, G1.4, Prague ,1998.